ELSEVIER

Journal of Alloys and Compounds 330–332 (2002) 414–419

Journal of ALLOYS AND COMPOUNDS

www.elsevier.com/locate/jallcom

Short-lived 'Schrödinger's cat' states of protons in metal–hydrogen systems: a new effect

C.A. Chatzidimitriou-Dreismann[a,*], T. Abdul-Redah[a], J. Sperling[b]

[a] *I.N. Stranski-Institute, Technische Universität Berlin, Strasse des 17 Juni 112, D-10623 Berlin, Germany*
[b] *Department of Solar Energetics, Hahn-Meitner-Institute, Glienicker Strasse 100, D-14109 Berlin, Germany*

Abstract

Recent neutron Compton scattering (NCS) investigations on niobium and palladium hydrides at ambient temperatures are reviewed. These experiments were motivated by (i) our previous theoretical work on short-lived quantum entanglement (QE) of protons in condensed matter, and (ii) our first experimental verification of this new effect with NCS from liquid H_2O/D_2O mixtures. All these NCS experiments revealed a striking anomalous behaviour of the total neutron scattering cross-section densities of protons, in the sub-femtosecond time scale. Whereas at small scattering angles the ratio of the cross-section of protons with respect to that of the metals corresponded to conventional theory, an 'anomalous' decrease was observed for increasing angles. Based on the fundamental van Hove theory, a first-principles theoretical interpretation of this novel effect is presented which takes explicitly into account QE of protonic states and its decoherence.

Keywords: Metallic hydrides; Neutron Compton scattering; Protons; Quantum entanglement; Mass interference; Sub-femtosecond dynamics

1. Introduction

The striking effect of quantum entanglement (QE) between states of two or more quantum systems, and the associated Einstein–Podolsky–Rosen (EPR) correlations, have been always considered to represent a striking feature of quantum theory [1]. Entangled states are often called Schrödinger's cat states. After the discovery of Bell's inequalities [2], which for the first time made possible the experimental test of QE and EPR correlations, a large number of basic experiments have confirmed the existence of QE in an impressive way. These experiments, however, usually deal with spatially well separated pairs of quantum systems (pairs of photons, atoms or ions) which are very well isolated from their environment. The latter condition is necessary due to the so-called decoherence (cf. Ref. [3]). In short, the process of decoherence refers to the suppression of quantum interference due to the 'disturbances' (or: dephasing) of the entangled particle states by the environment. Besides their importance for fundamental quantum mechanics, multiparticle QE and decoherence are also in the focus of several fast developing experimental and theoretical fields, e.g. quantum optics, quantum computation, quantum cryptography, etc.; cf. the Nobel symposium proceedings [4] and the book [5].

In condensed matter at ambient experimental conditions, however, QE and/or EPR correlations are usually considered to play no role and/or to be not accessible by experiment, due to the fast decoherence process [3]. In contrast, our previous theoretical investigations [6] concerning a novel short-lived QE of protons (and other light particles) in condensed systems have indicated that QE might be experimentally accessible by applying sufficiently 'fast' scattering techniques.

Our experimental work for the investigation of this new quantum effect in condensed matter started 1995, applying the neutron Compton scattering (NCS) method on water [7,8]. Since then, further systems investigated have been polymers [9], liquid benzene (in preparation), and metallic hydrides (in collaboration with E. Karlsson) [10,11]. These various successful experiments provided strong direct evidence for QE of protons in the time scale of ca. $10^{-16} - 10^{-15}$ s. One striking result of these experiments is that the total neutron scattering cross-section density of protons exhibits a very strong 'anomalous' decrease, in

*Corresponding author. Tel.: +49-30-314-22692; fax: +49-30-314-26602.

E-mail address: dreismann@chem.tu-berlin.de (C.A. Chatzidimitriou-Dreismann).

0925-8388/02/$ – see front matter
PII: S0925-8388(01)01649-8

some cases even by ca. 30% [7–11]. In this paper we consider the previous NCS experiments on metallic hydrides and provide a concise theoretical interpretation of the considered QE effect, which is based on the fundamental neutron scattering formalism of van Hove [12].

2. NCS experimental procedure

We have investigated the NCS process from niobium hydrides [10] and palladium hydrides [11] with various H and D contents. In this paper, the focus is particularly on the Nb–H and Pd–H systems. The NCS experiments were performed with the aid of the electron volt spectrometer eVS of the ISIS neutron spallation source, Rutherford Appleton Laboratory, UK.

For our purposes, the NCS technique [13] is particularly suitable, because the scattering time — i.e. the interaction time of the (epithermal) neutrons with the scattering nuclei — is sufficiently short, being in the sub-femtosecond time scale [8–10]. This is a consequence of the large energy (say, 3–150 eV) and momentum transfers (say, 10–300 $Å^{-1}$), applied at the eVS instrument. Moreover, for the same reason, the recoil peaks of H, D, and the other heavier atoms (e.g. Nb, Pd and Al) in the directly measured time-of-flight (TOF) spectra are well separated for a wide range of scattering angles; cf. Fig. 1. This fact is crucial for the precision and reliability of our experiments because it makes possible the direct determination of the ratio A_H/A_X of the areas under the recoil peaks of H and X (with X = Nb, Pd, etc.). The areas of the recoil peaks are determined incorporating the well known correction for the kinematic angle dependence of scattering intensities [9,10,13]. According to well established theory, under the prevalent conditions of NCS, the equation

$$A_H/A_X = N_H\sigma_H/N_X\sigma_X \quad (1)$$

must be strictly valid [8]. N_H/N_X is the ratio of the particle number densities of H and X, which is precisely known through sample preparation. σ_H and σ_X are the total neutron scattering cross-sections of H and another atom X. Thus, since the conventionally expected values of σ_H and σ_X are given in standard tables, the validity of Eq. (1) is immediately subject to experimental test.

TOF spectra were recorded for each of the available 32 detectors separately. For a detailed account of the eVS instrument and the standard procedure of data analysis (see, e.g. Refs. [13,9]). Here, it should be pointed out that only the heights — but not the positions and the widths of the recoil peaks — are fitting parameters. [The position of a peak is determined by energy and momentum conservation of the neutron–nucleus collision; the peak width is determined by the momentum distribution of the nucleus in the electronic potential of its chemical bond, together with its instrumental resolution function.] This fact (i.e. the reduction of the three possible fitting parameters to just one) facilitates the data analysis, and increases the reliability of the obtained results, considerably [7–11].

To prevent a possible source of confusion, it should be stressed that the data analysis procedure already incorporates the well known transformation from the 'free atom' to the 'bound atom' cross-section, i.e. $\sigma_{bound} = \sigma_{free} \cdot (1 + m/M)^2$ (M, atom mass; m, neutron mass) which is particularly relevant for light nuclei, like H. The results presented in the following sections make use of 'bound atom' cross-sections, which is in agreement with standard nomenclature of NCS investigations.

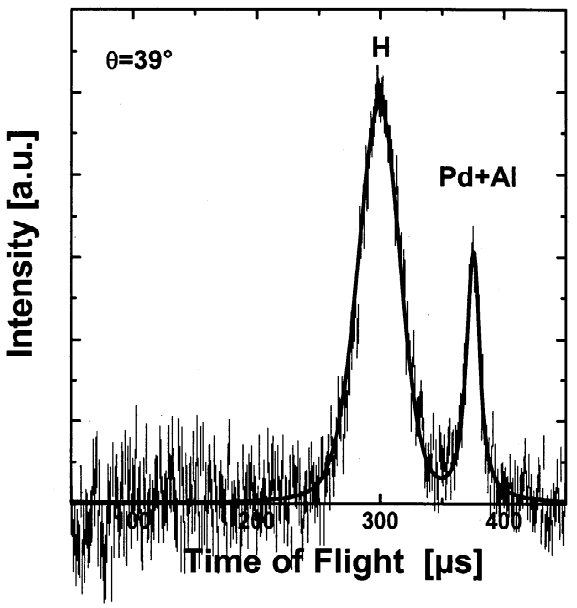

Fig. 1. A time-of-flight (TOF) spectrum of $PdH_{0.5}$, for the scattering angle $\theta = 39°$. Solid line, theoretical fit to the data; error bars, one standard deviation due to counting statistics. The sample was at room temperature. As shown in the figure, the Pd and Al recoil peaks (the latter being due to the container) overlap. For scattering angles $\theta > 100°$, the Pd and Al recoil peaks are resolved; cf. the text.

3. NCS results

Let us consider our NCS experimental results on the niobium hydride $NbH_{0.85}$ [10]. The Nb hydride samples have the advantage that they can be made in the form of foils. Thus there is no need of containers (cf. below). A thin oxide layer on the surface of the Nb foils prevents hydrogen desorption below 450°C. The Nb foils were about 0.5-mm thick. Various experimental tests and Monte Carlo simulations have shown that multiple scattering effect are sufficiently small for our purposes, i.e. they may affect the H/Nb areas of the TOF spectra by about 1% [10]. Experiments were done for various temperatures between 20 and 300 K.

Our NCS experiments on this system revealed a striking

dependence of σ_H/σ_{Nb} on the neutron scattering angle, and equivalently, on the characteristic time (i.e. the so-called scattering time, see Eq. (3) below) of the neutron–proton scattering process [10]; cf. Fig. 2. These results are discussed below, in connection with the related results from palladium hydride.

Our second experiment on metallic hydrides were performed on various protonated and deuterated palladium hydrides [11]. Here let us consider the results from $PdH_{0.5}$. The Pd-foils used were about 0.5-mm thick. The foils were hydrogenated in situ directly before measurement. In contrast to the niobium hydrides, these samples were kept in an Al container inside the gassing equipment at constant pressure during the measurements, since hydrogen desorbs at room temperature and normal pressure.

Two detector banks, containing eight neutron detectors each, were set in the forward scattering direction (scattering angle: $30° < \theta < 80°$). Eight detectors were set in the backward scattering direction ($107° < \theta < 125°$). Due to the high energy transfers in the backward scattering a reasonable separation of the palladium recoil peak from that of the aluminium one (due to sample container) was achieved. This allowed the determination of the ratio of the Pd to the Al scattering contributions. This ratio was then used to correct for the Al scattering of the forward direction when extracting the Pd-contribution to the signal area. Then, the areas A_i of the scattering signal due to H (after the appropriate data reduction) were divided by the Pd areas and normalized to the number density N_i of the particles existing in the sample (known from the phase diagram and the pressure adjustment during the gassing procedure). This gave the scattering cross-section ratios

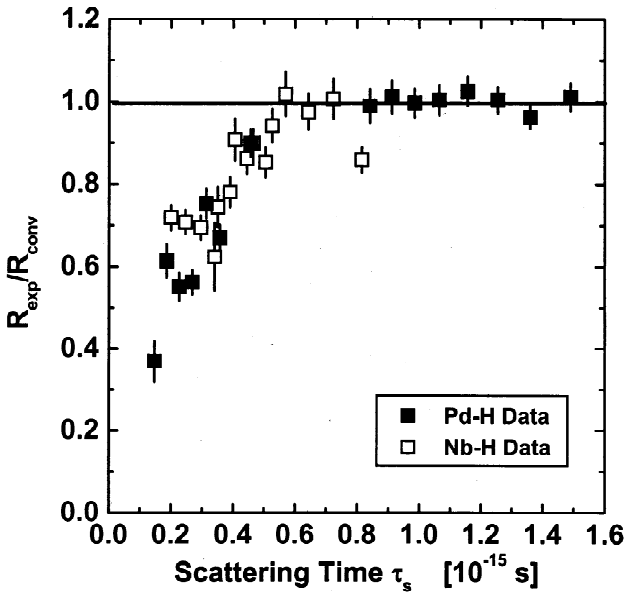

Fig. 2. Full symbols: the experimentally determined ratio $R_{exp} = \sigma_H/\sigma_{Pd}$, divided by its conventionally expected value $R_{conv} = 16.0$, as a function of scattering time τ_{scatt}. Open symbols: the corresponding quantity R_{exp}/R_{conv} for the Nb–H data, with $R_{conv} = 13.1$ (adapted from Ref. [11]).

$$R = \frac{\sigma_i}{\sigma_j} = \frac{A_i/N_i}{A_j/N_j} \tag{2}$$

according to Eq. (1). The ratios were determined for each detector separately.

As in the case of the Nb–H system, the experiments revealed again a striking dependence of σ_H/σ_{Nb} on the neutron scattering angle, and equivalently, on the scattering time of the neutron–proton scattering process [11]; cf. Fig. 2.

Here it is appropriate to give the relation of the scattering angle θ with the scattering time τ_{scatt} of the neutron–proton collision process under consideration. As shown by Sears [14] and Watson [15], τ_{scatt} is given by the relation

$$\tau_{scatt} = \frac{\hbar}{q(\theta)v_0} \tag{3}$$

where v_0 is the root-mean-square velocity of the proton before collision, and $q(\theta)$ is the momentum transfer; see also [9,10].

The results of both experiments for the τ_{scatt}-dependence of the cross-sections are shown in Fig. 2. Although the data for $R(\theta)$ do not follow the same curve for Pd–H and Nb–H, when $R(\tau_{scatt})$ is plotted, they turn out to be very similar. To show this, a normalization of R with respect to the conventionally expected values $(\sigma_H/\sigma_{Pd})_{conv} = 81.67/5.1 = 16.0$ and $(\sigma_H/\sigma_{Nb})_{conv} = 81.67/6.25 = 13.1$ is performed. The thus normalized results are presented in Fig. 2. Thus, after converting the angle dependence into scattering time dependence, according to Eq. (3), both niobium hydrides and palladium hydrides give the same $R(\tau_{scatt})$ dependence, although having different crystallographic features and/or electronic potentials at the H sites.

The above experimental results reveal the short-time dynamical character of the quantum entanglement under consideration. The considered effect was attributed to protonic quantum correlations [7–11], which, due to the very fast and effective decoherence process, are very short-lived in condensed matter. The NCS setup of ISIS probes time scales of the order of $10^{-16} - 10^{-15}$ s [8]; cf. Eq. (3).

The following observation is now crucial: In clear contrast to the above results, the total cross-section of H in water [8] and in a polymer (solid polystyrene) [9] revealed no angular — and, equivalently, scattering time — dependence of σ_H. As an example, the constancy of the scattering cross-sections of H and C observed in our NCS experiment from polystyrene foils is shown in Fig. 3. [Parenthetically, this constancy also demonstrates that the data analysis procedure takes into account the well known θ-dependence of the H-neutron scattering intensity in the laboratory system of reference.] This difference demonstrates that the local environmental interactions of the scattering H's play a significant role not only in the

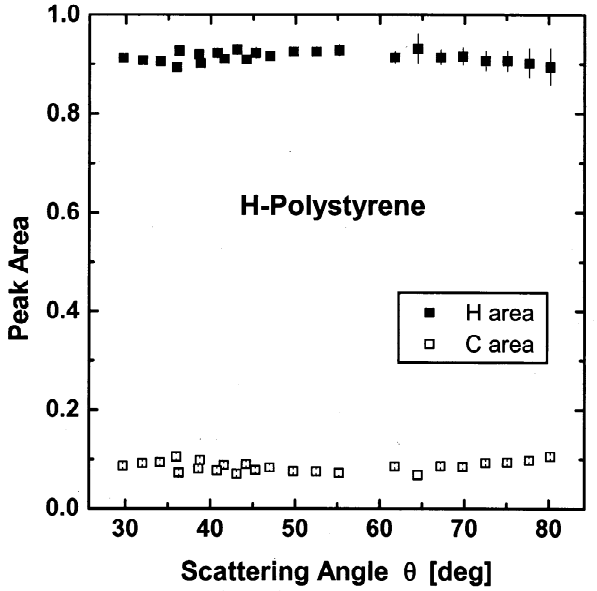

Fig. 3. The areas under the NCS recoil peaks of H and C from solid polystyrene (after correction for the well-known kinematic angle dependence; see the text and Ref. [9]). The stoichiometric composition of this compound is H:C = 1:1. The constancy of both recoil peak areas (which is in line with conventional theory) over the whole range of scattering angles should be observed.

conventional 'relaxation' processes, but also in the decoherence of the QE of the particles. In other terms (cf. the next section), the H-entanglement in water and in polystyrene has a decoherence time τ_{dec} being longer than the 'window' of scattering times τ_{scatt} presently implemented at the eVS instrument, whereas the τ_{dec} of the H's in the metals Nb and Pd apparently does not exceed the available τ_{scatt}-window. Indeed, Fig. 2 shows that the H-entanglement in the metallic hydrides effectively 'disappears' for scattering times larger than 0.6 fs.

Many efforts were spent on the search for possible trivial effects that could be responsible for the anomalous effects observed. Since the metallic foils were arranged perpendicular to the incoming beam the objection could be raised that multiple scattering effects could lead to a decrease of the H area at high angles due to multiple scattering. However, rotating the sample by ca. 30° gave the same angular dependence of the ratio *R*. Furthermore, most recent investigations have shown that possible dead time effects of the used detectors cannot account for the striking effect under consideration.

4. Theoretical interpretation

In this section, a concise theoretical interpretation of the 'anomalous' NCS effect under consideration is presented; cf. [9]. The theoretical approach is based on the fundamental van Hove theory of neutron scattering [12], and its specialization to the context of NCS. The corresponding notations and derivations follow the presentation of Watson [15].

The starting point is the basic formula for the double differential cross-section, which, for N identical nuclei, reads

$$\frac{\mathrm{d}^2\sigma}{\mathrm{d}\Omega'\,\mathrm{d}\epsilon'} = Nb^2\frac{k'}{k}S(q,\omega). \tag{4}$$

b is the bound scattering length of the nuclei. According to (1), the scattered intensity is proportional to the dynamic structure factor (or, response function) $S(q,\omega)$. $\hbar q$ and $\hbar\omega$ are the momentum and energy transfers that are transferred from the neutron to the scattering particle in the collision. Under the prevalent NCS physical conditions one finds [14,15]

$$S(q,\omega) = \hbar^{-1}\langle\delta(\omega - \omega_R - \mathbf{q}\cdot\mathbf{P}/M)\rangle, \tag{5}$$

which follows from the correlation function

$$Y(q,t) = \langle\exp[i(\mathbf{q}\cdot\mathbf{P}/M + \omega_R)t]\rangle \tag{6}$$

by time-Fourier transformation. $\omega_R = \hbar q^2/2M$ is the (free-atom) recoil frequency, $\mathbf{P}$ is the momentum operator of the nucleus (with mass M) and δ is the Dirac delta function. In these expressions,

$$\langle\cdots\rangle \equiv \sum p_n\langle\Psi_n|\cdots|\Psi_n\rangle, \tag{7}$$

is the appropriately combined quantum and thermodynamic average related with the condensed matter system (with states Ψ_n occurring with probabilities p_n).

Here it may be helpful to stress the following points:

(a) Ψ_n do *not* represent 'one-particle' states, but 'many-particle' states of the condensed system [12,14,15]. This implies immediately that, if necessary, quantum correlations between particles are incorporated into these states. For example, in an idealized model assuming entanglement between identical protons (representing scatterers), the quantum correlations due to the identity of the protons — i.e. the so-called exchange correlations — are represented by properly antisymmetrized state functions Ψ_n.

(b) Of course, the quantity $\mathbf{P}$ appearing in Eqs. (5) and (6) is a one-body operator [14,15]. Therefore, one could erroneously be inclined to interpret these equations as representing 'simply the scattering of neutrons by *single* nuclei (e.g. single protons)'. Obviously, the many-body character of Ψ_n (especially for entangled scatterers) definitely rules out this possibility.

In every conventional theoretical treatment, the scattering nuclei are tacitly assumed to show no QE and/or decoherence, and the average $\langle\cdots\rangle$ leads straightforwardly to the very well known and widely applied result

$$S(q,\omega) = \hbar^{-1}\int n(\mathbf{p})\,\delta(\omega - \omega_R - \mathbf{q}\cdot\mathbf{p}/M)\,\mathrm{d}\mathbf{p} \tag{8}$$

which relates the measured scattering spectra directly to the momentum distribution $n(\mathbf{p})$ of the scattering nuclei [14,15].

For the interpretation of the 'anomalous' NCS effect presented in the previous section, the following point is crucial. If QE of a scattering nucleus (say A, at position r_A) with another one (say B, at position r_B) does exist, the basic Eq. (8) may be violated. To prove this surprising statement, let us consider one *arbitrarily* chosen term

$$\exp(i\omega_R t)\langle\Psi_n|\exp[i(\mathbf{q}\cdot\mathbf{P}/M)t]|\Psi_n\rangle \tag{6a}$$

of $Y(q,t)$, and put explicitly $\Psi_n = \Psi_n(r_A, r_B, \dots)$. [As mentioned above, Ψ_n takes into account all necessary symmetries and/or correlations of many-body quantum systems associated with identical particles.] If A and B are spatially entangled, then Ψ_n does *not* factorize into a product of two factors like $\Psi_{nA}(r_A, \dots) \otimes \Psi_{nB}(r_B, \dots)$. It is expected that this QE will have a 'short' lifetime, called decoherence time, τ_{dec} [3]. Defining the associated pure-state density operator $\rho_n = |\Psi_n\rangle\langle\Psi_n|$ and introducing the reduced density operator being relevant for the scatterer A by $\rho_A = \mathrm{Tr}_{(r_B, \dots)}\rho_n$, one has

$$\begin{aligned} Y_{nn}(t) &= \langle\Psi_n|\exp[i(\mathbf{q}\cdot\mathbf{P}/M)t]|\Psi_n\rangle \\ &= \mathrm{Tr}(\rho_A \exp[i(\mathbf{q}\cdot\mathbf{P}/M)t]). \end{aligned} \tag{9}$$

At this stage, the time-evolution of ρ_A, due to decoherence of $|\Psi_n\rangle$, will be introduced into the formalism explicitly. It should be stressed that decoherence is a non-unitary process. Indeed, this holds for all well-known dynamical equations describing decoherence — as formulated, e.g. by Caldeira and Leggett, Zurek, Joos and Zeh, Lindblad, and others [3]. To be concrete, in the following we will use the theoretical treatment of Joos and Zeh [3a,3f]. Their equation of motion for the reduced density operator $\rho_A(t)$ reads

$$i\hbar\,\partial\rho_A/\partial t = [H, \rho_A] - i\,\Lambda[x,[x,\rho_A]] \tag{10}$$

where H is the relevant (or effective) Hamiltonian of the particle, and Λ is a positive constant called 'localization rate'. This dynamical equation describes positional entanglement [3]. The solution of Eq. (10) in the position representation, $\langle x|\rho_A(t)|x'\rangle \equiv \rho_A(x,x',t)$, is

$$\rho_A(x,x',t) = \rho_A(x,x',0)\exp[-\Lambda(x-x')^2 t]. \tag{11}$$

Expressing Eq. (9) in the position representation,

$$Y_{nn}(t) = \int\int \mathrm{d}x\,\mathrm{d}x' \langle x|\rho_A(t)|x'\rangle\langle x'|\exp[i\,t\,\mathbf{q}\cdot\mathbf{P}/M]|x\rangle, \tag{12}$$

and using Eq. (11), some straightforward calculations lead to the result [9]

$$\begin{aligned} Y_{nn}(t) = \int\int\int \mathrm{d}\mathbf{p}\,\mathrm{d}x\,\mathrm{d}x'\, C(x,x',\mathbf{p})\,\exp[-\Lambda(x-x')^2 t] \\ \cdot \exp[i\,t\,\mathbf{q}\cdot\mathbf{p}/M]. \end{aligned} \tag{13}$$

$C(x,x',\mathbf{p})$ is an explicitly given function of the denoted arguments; $\mathbf{p}$ is an eigenvalue of the momentum operator $\mathbf{P}$.

It is interesting to note that, besides the oscillatory function $\exp[i\,t\,\mathbf{q}\cdot\mathbf{p}/M]$ of Eqs. (6) and (6a), Eq. (13) exhibits the additional factor $\exp[-\Lambda(x-x')^2 t]$ which is due to QE and decoherence. This factor is less than one for every time $t \neq 0$ and thus causes an 'anomalous' decrease of $Y_{nn}(t)$, which is unknown in the frame of standard theory. Recall that $Y_{nn}(t)$ was arbitrarily chosen and thus the result Eq. (13) holds for all states Ψ_n. Inserting $Y_{nn}(t)$ into $Y(q,t)$ one sees that also $Y(Q,t)$ decreases 'anomalously'. Therefore, the t-Fourier transform of $Y(q,t)$ — which gives $S(q,\omega)$ — as well as the total cross-section — which is defined by an integral over ω of $S(q,\omega)$ — must exhibit this 'anomalous' decrease, too [9].

5. Discussion

The following point may be worth mentioning. A total cross-section, by definition, is proportional to the frequency (ω) integral of the dynamic structure function $S(q,\omega)$. In standard theoretical treatments, where decoherence plays no role, this integral is trivially proportional to the ω-Fourier transform of $S(q,\omega)$ at time $t = 0$, i.e. to $Y(q,t=0)$. But if QE and decoherence are present, then there is an additional t-dependence in $Y(q,t)$ which has nothing to do with the factor $\exp(i\omega t)$ of the Fourier transforms, but is caused by the physical process of decoherence, as our preceding treatment has shown. Thus, the trivial substitution $t = 0$ in $Y(q,t)$ is not equivalent with the ω-integral over $S(q,\omega)$ any more.

Clearly the considered QE effect (firstly observed in liquid water [7,8] and later in metallic hydrides [10,11] and in polymers [9]) cannot be observed with 'very slow' techniques, like e.g. neutron interferometry [16]. Additionally, motivated by these experimental NCS results, this effect has been recently considered theoretically in Ref. [17], using a method independent of the van Hove theory. However, QE between (pairs of) protons and/or deuterons plays a crucial role in [17], too.

It is also interesting to note that entanglement between pairs of adjacent protons has been shown to strongly affect the proton transfer and/or vibrational dynamics in the molecular crystal $KHCO_3$, in particular applying the method of incoherent elastic neutron scattering [18,19].

Let us consider the theoretical derivations in cases (like, e.g. liquid He below the superfluid transition temperature) where the decoherence time τ_{dec} is 'infinite' or very much larger than the scattering time τ_{scatt}; i.e.: $\tau_{\mathrm{dec}} \gg \tau_{\mathrm{scatt}}$. This implies that the additional factor $\exp[-\Lambda(x-x')^2 t]$ in Eq. (13) becomes equal to 1. Therefore, in the present case the considered 'anomalous' QE effect does not exist.

The above considerations lead to the conclusion that the new effect under consideration may become observable in

a suitable 'decoherence time window' only, viz. when $\tau_{dec} \sim \tau_{scatt}$. According to this conclusion, the results presented in Fig. 2 show how this time window starts to 'open' as the scattering time given by the experimental set-up (i.e. in essence the scattering angle and the associated large momentum transfer) decreases from 1.5 to 0.2 fs.

The presented results strongly affect the conventional and widely used theoretical concept of electronic Born–Oppenheimer (BO) potential energy surfaces. Recall that BO surfaces are determined by considering the nuclei as classical mass points and fixing them at various spatial configurations, which allows then to solve the associated 'electronic' Schrödinger equations. As a matter of fact, our results clearly demonstrate that the protons in metallic hydrides (and other systems) cannot be described as classical mass points in the sub-femtosecond time scale. This conclusion may also have considerable multidisciplinary implications, since this time scale is of the order of the characteristic time of the electronic rearrangements accompanying (i) the formation and/or breaking of a typical chemical bond in a molecule, or (ii) positional changes of protons in a metallic lattice.

Acknowledgements

We thank E.B. Karlsson, J. Mayers and R.M.F. Streffer for close collaboration and helpful discussions. C.A.C.-D. acknowledges partial support by the Fonds der Chemischen Industrie (Frankfurt) and by a grant from the Royal Swedish Academy of Sciences (Stockholm).

References

[1] A. Einstein, B. Podolsky, N. Rosen, Phys. Rev. 47 (1935) 777.
[2] J.S. Bell, Physics 1 (1964) 195.
[3] (a) D. Giulini, E. Joos, C. Kiefer, J. Kupsch, I.-O. Stamatescu, H.D. Zeh, in: Decoherence and the Appearance of a Classical World in Quantum Theory, Springer, Berlin, 1996;
(b) R. Omnès, in: The Interpretation of Quantum Mechanics, Princeton University Press, Princeton, 1994;
(c) W.H. Zurek, Physics Today 44 (10) (1991) 36;
(d) S. Haroche, Physics Today 51 (7) (1998) 36;
(e) A.O. Caldeira, A.J. Leggett, Physica A 121 (1983) 587;
A.O. Caldeira, A.J. Leggett, Phys. Rev. A 31 (1985) 1059;
(f) E. Joos, H.D. Zeh, Z. Phys. B: Condens. Matter 59 (1985) 223.
[4] Proceedings of the Nobel Symposium 104, Modern Studies of Basic Quantum Concepts and Phenomena, in: E.B. Karlsson, E. Brändas (Eds.), Physica Scripta, Vol. T76 (1998).
[5] D. Bouwmeester, A. Ekert, A. Zeilinger (Eds.), The Physics of Quantum Information, Springer, Berlin, 2000.
[6] C.A. Chatzidimitriou-Dreismann, Adv. Chem. Phys. 80 (1991) 201;
C.A. Chatzidimitriou-Dreismann, Adv. Chem. Phys. 99 (1997) 393.
[7] C.A. Chatzidimitriou-Dreismann, J. Mayers, Physica B 226 (1996) 231.
[8] C.A. Chatzidimitriou-Dreismann, T. Abdul-Redah, R.M.F. Streffer, J. Mayers, Phys. Rev. Lett. 79 (1997) 2839.
[9] C.A. Chatzidimitriou-Dreismann, T. Abdul-Redah, J. Sperling, J. Chem. Phys. 113 (2000) 2784.
[10] E.B. Karlsson, C.A. Chatzidimitriou-Dreismann, T. Abdul-Redah, R.M.F. Streffer, B. Hjörvarsson, J. Öhrmalm, J. Mayers, Europhys. Lett. 46 (1999) 617.
[11] T. Abdul-Redah, R.M.F. Streffer, C.A. Chatzidimitriou-Dreismann, B. Hjörvarsson, E.B. Karlsson, J. Mayers, Physica B 276–278 (2000) 824.
[12] L. Van Hove, Phys. Rev. 95 (1954) 249.
[13] J. Mayers, T.M. Burke, R.J. Newport, J. Phys.: Condens. Matter 6 (1994) 641.
[14] V.F. Sears, Phys. Rev. B 30 (1984) 44.
[15] G.I. Watson, J. Phys. Condens. Matter 8 (1996) 5955.
[16] C.A. Chatzidimitriou-Dreismann, T. Abdul-Redah, R.M.F. Streffer, B. Hessmo, Phys. Rev. Lett. 84 (2000) 2036.
[17] E.B. Karlsson, S.W. Lovesey, Phys. Rev. A 61 (2000) 062714.
[18] F. Fillaux, Physica D 113 (1998) 172.
[19] S. Ikeda, F. Fillaux, Phys. Rev. B 59 (1999) 4134.